Available online at www.sciencedirect.com
ScienceDirect
Dyes and Pigments 76 (2008) 775–783
DYES and PIGMENTS
www.elsevier.com/locate/dyepig

Azo dyes based on 8-hydroxyquinoline benzoates: Synthesis and application as colorimetric Hg^{2+}-selective chemosensors

Yunfei Cheng, Meng Zhang, Hong Yang, Fuyou Li*, Tao Yi, Chunhui Huang*

Department of Chemistry and Laboratory of Advanced Materials, Fudan University, Shanghai 200433, PR China

Received 16 December 2006; received in revised form 25 January 2007; accepted 25 January 2007
Available online 12 April 2007

Abstract

A series of 8-hydroxyquinoline benzoates with diverse azo substituents were synthesized by diazo-reaction of 2-methyl-8-hydroxyquinoline with some arylamines, followed by esterification with benzoyl chloride. All the products allowed selective sensing with Hg^{2+}, which was affirmed by UV–vis absorption spectra. Different spectral changes were observed for these compounds with electron-donating substituent (bathochromic shift) or electron-withdrawing substituent (hypsochromic shift). Particularly, obvious color change was observed for 5-(4-dimethylaminophenylazo)-2-methylquinolin-8-yl benzoate in the presence of Hg^{2+}, which made it possible for distinguishing Hg^{2+} from other metal ions by naked eye.

Keywords: Azo dyes; 8-Hydroxyquinoline benzoates; Colorimetric Hg^{2+}-selective chemosensor

1. Introduction

Design and synthesis of new chemosensors for metal ions are important subjects in the field of supramolecular and material chemistry due to their fundamental role in biological, environmental and chemical processes [1]. As a dangerous and widespread global pollutant, mercury causes serious environmental and healthy problems because marine aquatic organisms convert inorganic mercury into neurotoxic methylmercury, a potent neurotoxin that bioaccumulates through the food chain. Subsequent ingestion of methylmercury by humans is connected to serious sensory, motor, and cognitive disorders. Therefore, it is important to explore new methods for monitoring Hg^{2+} [2]. Over the past years, many examples for mercury detection, including chromogenic [3] and fluorescent [4] chemical sensors, electrochemical devices [5], biosensors [6], and sensors based on mass changes [7] have been reported. Currently, colorimetric sensors are popular due to their capability to detect analyses by naked eye without resorting to any expensive instruments [8]. Therefore, to develop simple-to-use and naked-eye diagnostic tool, great efforts have been made for the design and synthesis of selective chromogenic sensors for Hg^{2+} [9].

8-Hydroxyquinoline benzoates have been adopted as receptors for Hg^{2+} [10]. However, their absorption spectral changes in ultraviolet (UV) region restrained their practical applications. At the same time, azo dyes have usually been used as colorimetric sensors for cations or anions for their strong chromogenic ability [1h,11]. The strong receptor–ion interaction can cause the absorption band of azo dye shift to visible light region in the presence of a certain ion [12]. Recently, we have reported that azo derivative 5-(4-dimethylaminophenylazo)-2-methylquinolin-8-yl benzoate could recognize Hg^{2+} [13]. In this paper, a series of azo 8-hydroxyquinoline benzoates **2–4** (see Scheme 1) with various azo substituents, such as electron-donating group ($-OCH_3$, $-N(CH_3)_2$) or electron-withdrawing

* Corresponding authors.
E-mail addresses: fyli@fudan.edu.cn (F. Li), chhuang@fudan.edu.cn (C. Huang).

0143-7208/$ - see front matter © 2007 Elsevier Ltd. All rights reserved.
doi:10.1016/j.dyepig.2007.01.022

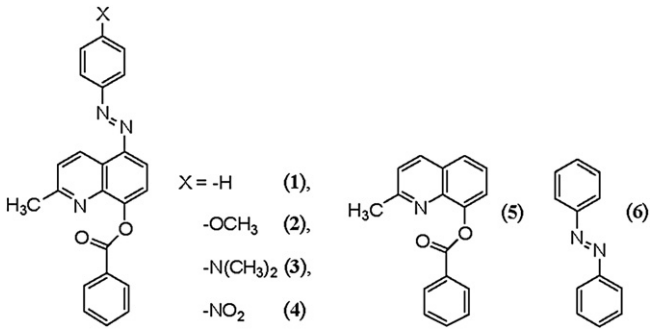

Scheme 1. Molecular structures of **1**–**6**.

group ($-NO_2$), were designed and synthesized. Furthermore, compounds **1**–**4** were characterized by single-crystal X-ray diffraction studies and could be used as colorimetric chemosensors for Hg^{2+}. For comparison, the photophysical properties of compounds **5** and **6** were also investigated.

2. Results and discussion

2.1. Single-crystal X-ray diffraction studies

Structural information of **1**–**4** were rendered by single-crystal X-ray diffraction studies. Molecular conformations of **1**–**4** are shown in Fig. 1. The corresponding crystal data and details of the structure determinations are given in Table 1. As expected, the steady structures of **1**–**4** are of *trans*-form in the crystals. Compound **1** crystallized in the monoclinic space group *P*2(1)/*c*, whereas **2**–**4** crystallized in the triclinic space group *P*-1, indicating that the substituents at 4-position of phenyl ring affect the crystal systems of these 8-hydroxyquinoline derivatives. Interestingly, compound **4** with electron-withdrawing substituent ($-NO_2$) exhibits two independent molecules with different bond lengths, bond angles and dihedral angles in the asymmetric unit cell in contrast to only one molecule for **1**–**3** (see ESI).

2.2. Photophysical properties

The data of UV–vis absorption spectra of **1**–**6** in CH_3CN (2.0×10^{-5} mol L^{-1}) are shown in Table 2. The maximal absorption wavelengths (λ_{max}) of **1**–**4** in CH_3CN are 350, 373, 445 and 376 nm, respectively, corresponding to the $\pi-\pi^*$ transition of the azo chromophores of **1**–**4**. Compared with λ_{max} of 2-methyl-8-hydroquinoline benzoate **5** (276 nm), λ_{max} of **1**–**4** are obviously red-shifted, indicating that the introduction of the $-N{=}N-$ group improves the chromogenic ability of the 8-hydroxyquinoline derivatives. Moreover, λ_{max} of **1**–**4** are bathochromically shifted in comparison with that of azobenzene **6** (316 nm), suggesting that the chromogenic ability of azobenzene derivatives could be improved by the presence of substituents. The maximal absorption wavelengths (λ_{max}) of **2** and **3** are red-shifted with reference to that of **1** in CH_3CN, which could be attributed to the stronger electron-donating abilities of $-OCH_3$ in **2** and $-N(CH_3)_2$ in **3**. Especially, the maximal absorption wavelength (λ_{max}) of **3** (445 nm) was modified successfully to visible light region. The molar absorption coefficients of **1**–**4** are 1.9×10^4 (350 nm), 2.0×10^4 (373 nm), 3.1×10^4 (445 nm) and 2.3×10^4 (376 nm) mol^{-1} L cm^{-1}, respectively (see Table 2), and are similar to that of **6** [2.2×10^4 mol^{-1} L cm^{-1} (316 nm)]. However, they are larger than that of **5** ($\varepsilon = 5.7 \times 10^3$ mol^{-1} L cm^{-1} at 276 nm), revealing that **1**–**4** have stronger ability of absorbing light than that of **5**.

2.3. Titration experiments of Hg^{2+}

The UV–vis spectrum is used extensively to study a coordination system with a spectral change, which is a convenient

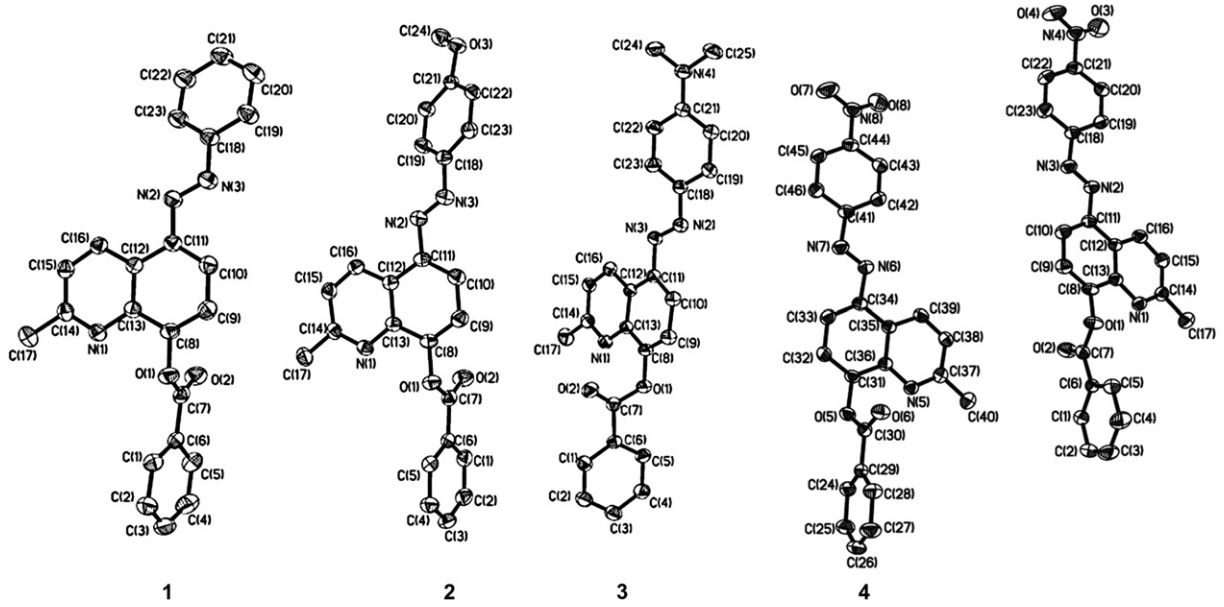

Fig. 1. Molecular conformations of **1**–**4**.

Table 1
Crystal data collection and structure refinement parameters for **1**–**4**

	1	**2**	**3**	**4**
Empirical formula	$C_{23}H_{17}N_3O_2$	$C_{24}H_{19}N_3O_3$	$C_{25}H_{22}N_4O_2$	$C_{23}H_{16}N_4O_4$
F_W	367.40	397.42	410.47	412.40
Crystal system	Monoclinic	Triclinic	Triclinic	Triclinic
Space group	*P*2(1)/*c*	*P*-1	*P*-1	*P*-1
Crystal size	0.15 × 0.10 × 0.08	0.20 × 0.15 × 0.15	0.35 × 0.20 × 0.05	0.35 × 0.25 × 0.20
a (Å)	11.727(2)	8.134(2)	8.773(1)	10.294(6)
b (Å)	8.796(2)	9.802(2)	9.726(2)	12.671(7)
c (Å)	18.247(4)	13.627(3)	13.207(2)	15.696(9)
α (°)	90	93.820(2)	107.738(2)	91.317(7)
β (°)	106.46(3)	100.250(2)	94.234(2)	98.785(7)
γ (°)	90	112.848(2)	98.989(2)	93.280(7)
V (Å)^3	1805.1(6)	974.0(3)	1051.2(3)	2019(2)
Z	4	2	2	4
ρ_{calcd} (g cm^{-3})	1.352	1.355	1.297	1.357
μ (mm^{-1})	0.088	0.091	0.085	0.096
F (000)	768	416	432	856
*R*1 [$I > 2\sigma(I)$]	0.0495	0.0376	0.0560	0.0443
*wR*2 [$I > 2\sigma(I)$]	0.1214	0.1023	0.1593	0.1225
GOF	0.973	1.075	1.049	1.042

method to determine the binding constants of the supramolecular complex [14]. In our present experiments, $Hg(ClO_4)_2$ was gradually added to the solution of **1**–**6** in CH_3CN as mercury source, and the complexation abilities of **1**–**6** with Hg^{2+} were investigated by the UV–vis absorption technique.

Fig. 2 shows UV–vis absorption spectra of **1** with various concentrations of Hg^{2+}. The characteristic strong absorption band of **1** at 350 nm decreased upon addition of Hg^{2+}, and a new band centered at 365 nm arose (see Fig. 2a), corresponding to a red-shift of the maximal absorption wavelength ($\Delta\lambda_{max} = 15$ nm), which indicated the formation of a new complex. The 1:1 binding stoichiometry between **1** and Hg^{2+} is supported by the nice nonlinear fitting [15] of the absorption-titration curve, which is also consistent with that reported in literature [10]. The binding constant *K* of **1** with Hg^{2+} was calculated to be 1.5×10^4 mol^{-1} L at 20 °C in CH_3CN solution (see Table 2). By comparison, the complexation abilities of **5** and **6** with Hg^{2+} were also observed upon addition of Hg^{2+} (see Fig. 2). When Hg^{2+} was added, the maximal absorption wavelength (λ_{max}) of **5** was shifted to 316 nm (see Fig. 2b), and no obvious change in the maximal absorption wavelength (λ_{max}) of **6** was observed (see Fig. 2c). These facts suggest that the presence of –N=N– group improves the chromogenic abilities of sensors for Hg^{2+}. At the same time, the binding site of **1** with Hg^{2+} is the 8-hydroxyquinoline benzoate section, not involved in –N=N– group.

Table 2
Photophysical properties of **1**–**6**

Compound	λ_{max}[a] (nm)	ε (mol^{-1} L cm^{-1})	λ_{max}[b] (nm)	$\Delta\lambda_{max}$[c] (nm)	*K*[d] (mol^{-1} L)
1	350	1.9×10^4	365	15	1.5×10^4
2	373	2.0×10^4	396	23	4.5×10^4
3	445	3.1×10^4	518	73	4.4×10^5
4	376	2.3×10^4	369	−7	3.3×10^4
5	276	5.7×10^3	316	40	$>10^3$
6	316	2.2×10^4	316	0	–

[a] In CH_3CN solution.
[b] Upon addition of Hg^{2+} in CH_3CN solution.
[c] $\Delta\lambda_{max} = \lambda_{max}{}^{b} - \lambda_{max}{}^{a}$.
[d] The binding constant *K* with Hg^{2+}.

Furthermore, the binding property of **1** for Hg^{2+} was also investigated by using ^1H NMR experiment in CD_3CN. Fig. 3 shows the ^1H NMR spectra of **1** before and after addition of 2.5 equiv. of Hg^{2+}. It is observed that significant downfield shifts of proton chemical shifts of the benzoate and quinolinyl groups of **1** with varied extent occurred in ^1H NMR spectra of **1** upon addition of Hg^{2+}, especially for that of proton in quinolinyl ring. For example, proton chemical shift of f changed to ca. 0.5 ppm. However, no obvious chemical shifts were observed for protons from a to e when Hg^{2+} was added. These facts indicate that the chelating site could be quinolinyl nitrogen atom together with ester oxygen atom. Moreover, proton signals of $-CH_3$ in quinolinyl ring shift downfield significantly from 2.63 to 3.06 ppm, which is similar to that of **5** (see ESI), further indicating that Hg^{2+} could interact with the 8-hydroxyquinoline benzoate section [10].

A similar red-shift of absorption band was observed when Hg^{2+} was added to the solution of **2** ($-OCH_3$) or **3** ($-N(CH_3)_2$) in CH_3CN (see Fig. 4). For example, upon addition of Hg^{2+}, the characteristic strong absorption band of **3** at 445 nm decreased, and a new band centered at 518 nm arose, corresponding to a λ_{max}(abs) red-shift of 73 nm and an isobestic point at 476 nm. As a result, an apparent color change from yellow to red in ambient light could be observed by naked eye (see Fig. 5). Furthermore, the binding constants *K* of **2** and **3** with Hg^{2+} were calculated to be 4.5×10^4 and 4.4×10^5 mol^{-1} L at 20 °C in CH_3CN solution, respectively (see Table 2).

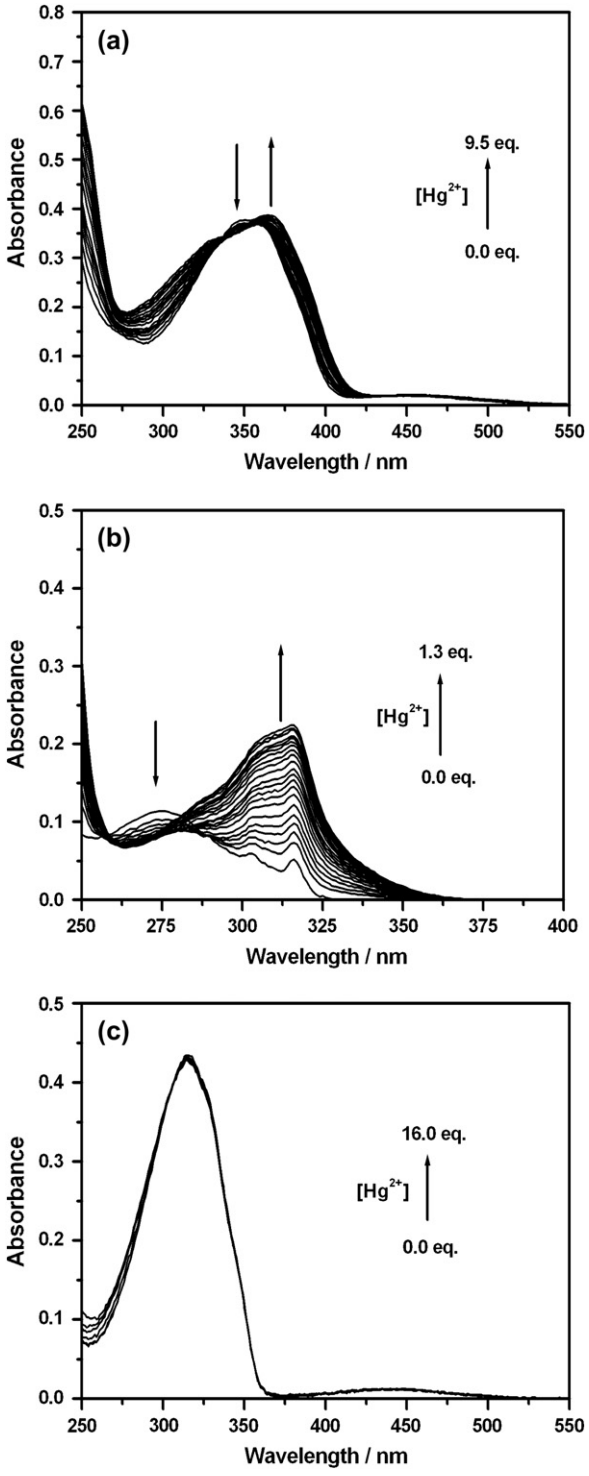

Fig. 2. UV–vis absorption spectra of **1** (a), **5** (b), and **6** (c) in CH_3CN ($[C] = 2.0 \times 10^{-5}$ mol L^{-1}) upon addition of Hg^{2+}.

Different phenomenon was observed for **4** with $-NO_2$ substituent when Hg^{2+} was added (see Fig. 4c). Upon addition of Hg^{2+} in the CH_3CN solution, the characteristic absorption band of **4** at 376 nm decreased, and a new band centered at 369 nm arose, corresponding to a blue-shift of the maximal absorption wavelength ($\Delta\lambda_{max} = 7$ nm). The different spectral change between **2** (or **3**) and **4** could be attributed to the different electron-donating and -withdrawing abilities of their substituents. The D–π–A structure exists in **4** with the strong electron-withdrawing group ($-NO_2$) (see Fig. 6). Here, nitro-substituted phenyl group ($PhNO_2$) is an electron-acceptor (A), and benzoate quinolinyl group is an electron-donor (D). Upon addition of Hg^{2+}, the complexation between Hg^{2+} and the quinolinyl nitrogen atom together with oxygen atom of **4** decreased the electron-donating ability of the donor, and then the D–π–A structure changed to A–π–A structure, which diminished the extent of intramolecular charge transfer (ICT) and resulted in the blue-shift of absorption band of **4** [16]. However, in comparison with **4**, the D–π–D structure exists in **2** or **3** with the electron-donating group ($-OCH_3$ or $-N(CH_3)_2$) and the relative weak donor (benzoate quinolinyl group) (see Fig. 6). The complexation of **2** or **3** with Hg^{2+} made benzoate quinolinyl group to be an electron-acceptor, and then the complexes **2**·Hg^{2+} or **3**·Hg^{2+} might be considered as D–π–A structure, which enhanced the degree of ICT and resulted in the red-shift of absorption band of **2** or **3** [16]. Therefore, the sensing ability of these sensors with Hg^{2+} could be optimized by varying electron-donating and withdrawing abilities of their substituents.

2.4. Selectivity

For an excellent chemosensor, high selectivity is a matter of necessity. The selective coordination studies of **1**–**4** were then extended to related heavy, transition, and main group metal ions by absorption spectroscopy. Titration profiles of **1**–**4** show that all hydroxyquinoline benzoate derivatives are selective for Hg^{2+} (see ESI). Moreover, it is interesting that the experimental phenomenon was distinct when Cu^{2+} was added to the CH_3CN solution of **3** [13]. The sensing process consisted of two processes (see ESI). In the first process, upon addition of less than 1.0 equiv. of Cu^{2+}, the color of **3** changed from yellow to pale red, which could be attributed to the weak reaction of Cu^{2+} with the quinolinyl nitrogen atom together with oxygen atom. When more than 1.0 equiv. of Cu^{2+} was added, Cu^{2+} could further interact with $-N{=}N-C_6H_4-N(CH_3)_2$ [17,18], which would diminish the extent of ICT and resulted in the blue-shift of absorption band with the color change from pale red back to colorless. However, for the other compounds (**1**, **2**, **4**), the second response process could not be observed obviously upon addition of Cu^{2+}. So it is speculated that the distinct phenomenon of **3** may be attributed to its special structure for the presence of the strong electron-donating group ($-N(CH_3)_2$).

By plotting the changes of **3** in the absorbance intensity at 515 nm as a function of metal ion concentration, diverse curves are obtained and shown in Fig. 7. Upon addition of 3.0 equiv. of metal ions, no obvious red-shift spectral responses were observed for Zn^{2+}, Cd^{2+}, Ni^{2+}, Co^{2+}, Cr^{2+}, Pb^{2+}, Ca^{2+}, Ag^{+}, K^{+} or Na^{+}. However, the addition of Hg^{2+} resulted in a prominent red-shift of absorption band, which suggested the high selectivity of **3** to Hg^{2+}. Moreover, competition experiments were performed in 5.0 equiv. of Hg^{2+}

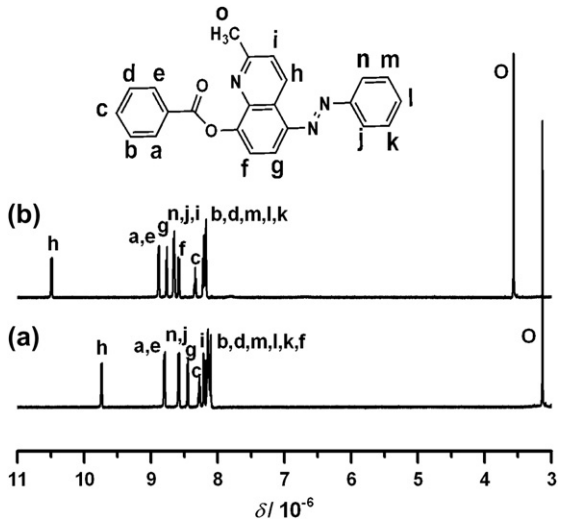

Fig. 3. ^{1}H NMR of **1** in CD_3CN before (a) and after (b) addition of 2.5 equiv. of Hg^{2+}.

mixed with 5.0 equiv. of background metal ions such as Zn^{2+}, Cd^{2+}, Ni^{2+}, Co^{2+}, Cr^{2+}, or Pb^{2+}. The data of spectral change in maximal absorption wavelength of **3** containing both background metal ions and Hg^{2+} showed similar variation in comparison with that containing only Hg^{2+} (see ESI). These facts indicated that **3** could be used as a colorimetric chemosensor for Hg^{2+}, as also shown in Fig. 5.

To explore practical applicability of **3** as a Hg^{2+}-selective sensor, H_2O was introduced to titration system of **3** for various metal ions. Fig. 8 shows UV–vis absorption spectra of **3** with 40.0 equiv. of representative metal ions in CH_3CN:H_2O = 9:1 (v/v). It can be seen from Fig. 8 that only the addition of Hg^{2+} resulted in an obvious red-shift (43 nm) of maximal absorption wavelength of **3**, which indicated that **3** could be used as colorimetric Hg^{2+} sensor in semi-aqueous sample.

3. Conclusions

In summary, we have presented a series of 8-hydroxyquinoline benzoates **1**–**4** with diverse azo substituents for Hg^{2+} sensors. The presence of –N=N– group improves the chromogenic ability of the chemosensors. It is also evident that bathochromic effect of **1**–**3** occurs as substituent changes from –H, $-OCH_3$, to $-N(CH_3)_2$ in CH_3CN solution. Upon complexation with Hg^{2+}, different spectral changes were observed for **2** and **3** with electron-donating group (bathochromic shift) and **4** with electron-withdrawing substituent (hypsochromic shift). Most importantly, **3** showed obvious color change from yellow to red in CH_3CN upon addition of Hg^{2+}. ^{1}H NMR spectra revealed that it was possible for the quinolinyl nitrogen atoms together with oxygen atoms in various reagent molecules to be the binding sites for Hg^{2+}. The design strategy presented in this paper would be of great interest in the development of other colorimetric sensors for metal ions.

4. Experimental

4.1. Instruments and reagents

All starting materials (aniline, 4-methoxyaniline, 4-dimethylaminoaniline, 2-methyl-8-hydroxyquinoline, benzoyl chloride) and compound **6** were obtained from Shanghai Chemical Reagent Company and used as received. All the metal ion sources in experiments were used by their nitrate salts except mercury of perchlorate. NMR spectra were recorded on a Mercury Plus 400NB NMR spectrometer or Bruker DMX-500 using TMS as an internal standard. UV–vis spectra were recorded with a UV–vis 2550 spectroscope (Shimadzu). MS (EI) spectra were recorded with a MA1212 mass spectroscope. The elemental analysis was performed with Vario EL III O-Element analyzer. Spectral titrations were carried out by injection of an aliquot of cation solution into receptor solution. Solution samples were measured in 1.00 cm quartz cell. Spectroscopic and colorimetric measurements were carried out in CH_3CN (HPLC) and deionized water.

4.2. Synthesis

Compounds **1**–**4** were synthesized by diazo-reactions of 2-methyl-8-hydroxyquinoline with diverse arylamines, respectively, followed by esterifications with benzoyl chloride. The structures of them were characterized by ^{1}H NMR, ^{13}C NMR spectra and MS (EI). Herein, only the synthesis of **1** is described in detail as an example.

4.2.1. Benzoic acid 5-phenylazo-2-methylquinolin-8-yl ester (1)

Aniline (0.093 g, 1 mmol) was suspended in 30.0 mL of distilled water at the temperature of 0–5 °C. Then 1.0 mL of 6.0 mol L^{-1} hydrochloric acid solution was added to the mixture. After 15 min, 10.0 mL aqueous solution of sodium

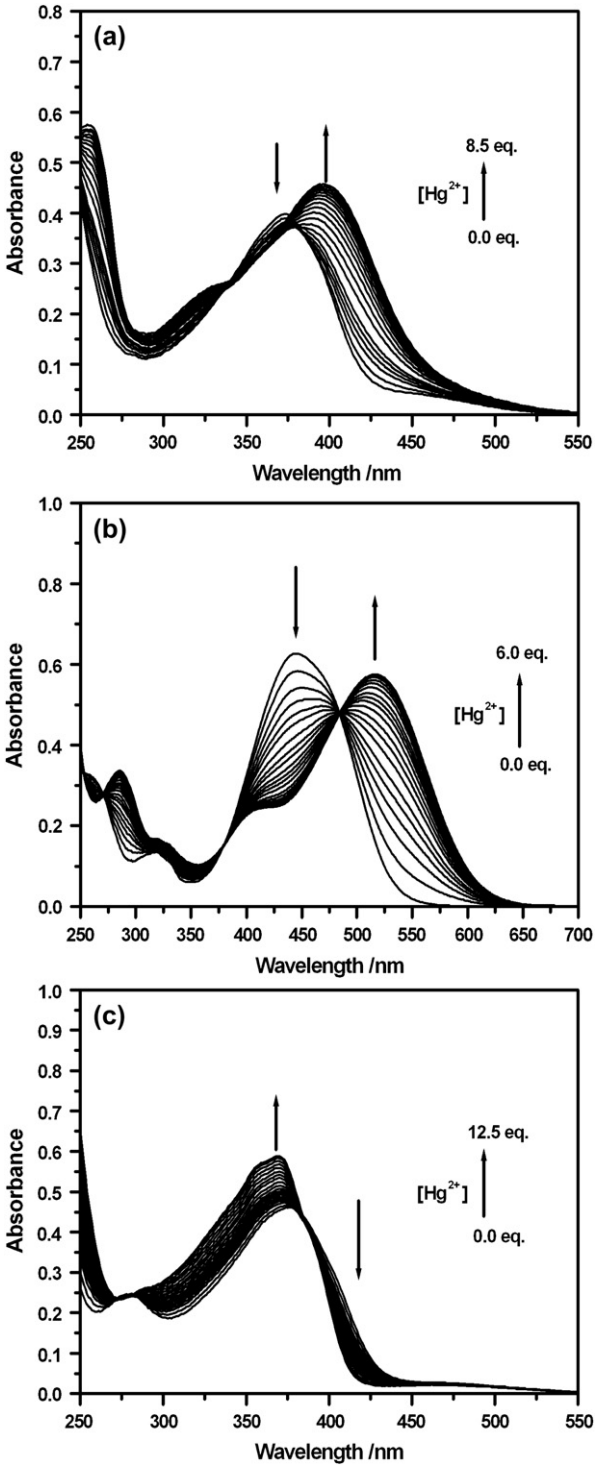

Fig. 4. UV–vis absorption spectra of **2** (a), **3** (b), and **4** (c) in CH_3CN ($[C] = 2.0 \times 10^{-5}$ mol L^{-1}) upon addition of Hg^{2+}.

nitrite (0.076 g, 1.1 mmol) was added, followed by acetonitrile solution of 2-methyl-8-hydroxyquinoline (0.159 g, 1 mmol), then pH was adjusted to 8–9 with 2.0 mol L^{-1} NaOH solution. After stirring for 2 h, the solution was neutralized with 1.0 mol L^{-1} HCl solution. The produced precipitate was filtered and washed several times with deionized water and dried at vacuum. Then 0.05 g of the product was refluxed with benzoyl chloride (0.057 g, 0.4 mmol) in CH_2Cl_2 (10 mL) for 6 h. The crude product was purified by silica column chromatography (petroleum ether (b.p. 60–90 °C)–chloroform, 1:4, v/v). Yield: 56%. ^{1}H NMR (400 MHz, $CDCl_3$, RT) δ: 9.18 (d, $J = 8.8$ Hz, 1H, ArH), 8.40 (t, 2H, ArH), 8.06 (t, 2H, ArH), 7.95 (d, $J = 8.0$ Hz, 1H, ArH), 7.70 (m, 1H, ArH), 7.65 (m, 1H, ArH), 7.60 (m, 5H, ArH), 7.47 (d, $J = 8.8$ Hz, 1H, ArH), 2.69 (s, 3H, CH_3). ^{13}C NMR (100 MHz, DMSO-d_6, RT) δ: 165.31, 160.66, 153.06, 150.03, 145.31, 140.88, 134.84, 132.84, 130.87, 130.29, 129.79, 129.55, 126.20, 124.70, 123.89, 122.52, 112.19, 26.04. MS (EI): $m/z = 367.4$ [M^+]. Anal. Calcd for $C_{23}H_{17}N_3O_2$ (367.13): C, 75.19; H, 4.66; N, 11.44. Found: C, 75.15; H, 4.60; N, 11.50.

*4.2.2. Benzoic acid 5-(4-methoxyphenylazo)-2-methylquinolin-8-yl ester (**2**)*

Yield: 50%. ^{1}H NMR (400 MHz, $CDCl_3$, RT) δ: 9.15 (d, $J = 8.8$ Hz, 1H, ArH), 8.38 (d, $J = 7.2$ Hz, 2H, ArH), 8.06 (m, 2H, ArH), 7.90 (d, $J = 8.4$ Hz, 1H, ArH), 7.70 (t, 1H, ArH), 7.62 (m, 3H, ArH), 7.44 (d, $J = 8.8$ Hz, 1H, ArH), 7.07 (d, $J = 8.8$ Hz, 2H, ArH), 3.92 (s, 3H, CH_3), 2.68 (s, 3H, CH_3). ^{13}C NMR (100 MHz, DMSO-d_6, RT) δ: 165.35, 163.13, 160.51, 149.34, 147.47, 145.47, 140.88, 134.80, 132.77, 130.67, 129.77, 129.60, 125.99, 125.92, 124.45, 122.51, 115.45, 111.80, 56.45, 26.04. MS (EI): $m/z = 397.3$ [M^+]. Anal. Calcd for $C_{24}H_{19}N_3O_3$ (397.14): C, 72.53; H, 4.82; N, 10.57. Found: C, 72.49; H, 4.76; N, 10.61.

*4.2.3. Benzoic acid 5-(4-dimethylaminophenylazo)-2-methylquinolin-8-yl ester (**3**)*

Yield: 46%. ^{1}H NMR (500 MHz, $CDCl_3$, RT) δ: 9.16 (d, $J = 8.6$ Hz, 1H, ArH), 8.38 (d, $J = 7.2$ Hz, 2H, ArH), 8.00 (d, $J = 8.6$ Hz, 2H, ArH), 7.86 (d, $J = 8.6$ Hz, 1H, ArH), 7.69 (t, 1H, ArH), 7.59 (m, 3H, ArH), 7.41 (d, $J = 8.6$ Hz, 1H, ArH), 6.81 (d, $J = 8.6$ Hz, 2H, AH), 3.13 (s, 6H, CH_3), 2.67 (s, 3H, CH_3). ^{13}C NMR (125 MHz, DMSO-d_6, RT) δ: 165.26, 159.23, 154.32, 151.81, 143.80, 142.23, 137.96, 135.28, 134.02, 130.35, 128.71, 123.97, 122.92, 122.61, 121.39, 114.68, 112.43, 40.38, 25.26. MS (EI): $m/z = 410.3$ [M^+]. Anal. Calcd for $C_{25}H_{22}N_4O_2$ (410.17): C, 73.15; H, 5.40; N, 13.65. Found: C, 73.10; H, 5.35; N, 13.69.

*4.2.4. Benzoic acid 5-(4-nitrylphenylazo)-2-methylquinolin-8-yl ester (**4**)*

Yield: 53%. ^{1}H NMR (400 MHz, $CDCl_3$, RT) δ: 9.15(d, $J = 8.4$ Hz, 1H, ArH), 8.44 (m, 2H, ArH), 8.38 (d, $J = 7.2$ Hz, 2H, ArH), 8.14 (d, $J = 9.2$ Hz, 2H, ArH), 8.01 (d, $J = 8.4$ Hz, 1H, ArH), 7.70 (t, 1H, ArH), 7.66 (d, $J = 8.0$ Hz, 1H, ArH), 7.60 (t, 2H, ArH), 7.49 (d, $J = 8.8$ Hz, 1H, ArH), 2.69 (s, 3H, CH_3). ^{13}C NMR (100 MHz, DMSO-d_6, RT) δ: 165.25, 160.90, 156.03, 151.17, 149.36, 145.204, 140.89, 134.89, 132.64, 130.72, 129.80, 129.48, 126.59, 125.79, 125.03, 124.71, 122.59, 112.89, 26.02. MS (EI): $m/z = 412.3$ [M^+]. Anal. Calcd for $C_{23}H_{16}N_4O_4$ (412.12): C, 66.99; H, 3.91; N, 13.59. Found: C, 66.93; H, 3.88; N, 13.62.

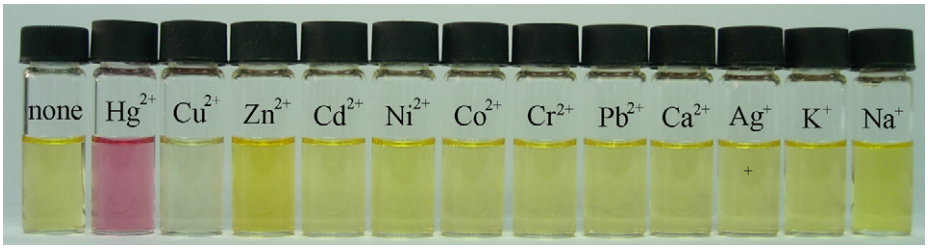

Fig. 5. The color changes of **3** in CH_3CN ($[C] = 2.0 \times 10^{-5}$ mol L^{-1}) upon addition of 4.0 equiv. of various metal ions.

*4.2.5. 2-Methyl-8-hydroquinoline benzoate (**5**)*

Compound (**5**) was synthesized by the procedure reported previously [10]. ^{1}H NMR (400 MHz, $CDCl_3$, RT) δ: 8.37 (d, $J = 7.2$ Hz, 2H, ArH), 8.07 (d, $J = 8.4$ Hz, 1H, ArH), 7.72 (m, 2H, ArH), 7.58 (m, 4H, ArH), 7.30 (t, 1H, ArH), 2.64 (s, 3H, CH_3). ^{13}C NMR (100 MHz, DMSO-d_6, RT) δ: 165.44, 159.74, 147.31, 140.72, 136.94, 134.61, 130.59, 129.82, 129.69, 128.16, 126.61, 126.11, 123.55, 122.37, 26.98. MS (EI): $m/z = 263.2$ [M^+]. Anal. Calcd for $C_{17}H_{13}NO_2$ (263.09): C, 77.55; H, 4.98; N, 5.32. Found: C, 77.46; H, 4.92; N, 5.37.

4.3. X-ray crystal structure determination

Crystallographic measurements of compounds **1**–**4** were carried out using a Bruker SMART CCD diffractometer, with σ scans and graphite-monochromated Mo Kα radiation ($\lambda = 0.71073$ Å) under room temperature. The structures were solved by direct methods and refined by full-matrix least-squares on F^2 values using SHELXS-97 program [19]. All non-hydrogen atoms were refined anisotropically. Hydrogen atoms were calculated in ideal geometries. For the full-matrix least-squares refinements [$I > 2\sigma(I)$], the unweighted and weighted agreement factors of $R1 = \sum(F_o - F_c)/\sum F_o$ and $wR2 = [\sum w(F_o^2 - F_c^2)^2/\sum wF_o^4]^{1/2}$ were used. CCDC reference numbers are 298218, 298739, 299042 and 298619 for **1**, **2**, **3** and **4**, respectively.

4.4. Calculations of binding constant

The binding constant K of 1:1 compound/Hg^{2+} complex formation calculated by the UV–vis absorption method is obtained by the following equation [20]:

$$A = A_0 + \frac{A_{\lim} - A_0}{2c_0}\left\{c_H + c_G + 1/K - \left[(c_H + c_G + 1/K)^2 - 4c_H c_G\right]^{1/2}\right\}$$

where A represents the ultraviolet absorbance; A_0 represents the absorbance of pure host; c_H and c_G are the corresponding concentrations of host and cation guest; c_0 represents the concentration of pure host; and K is the binding constant.

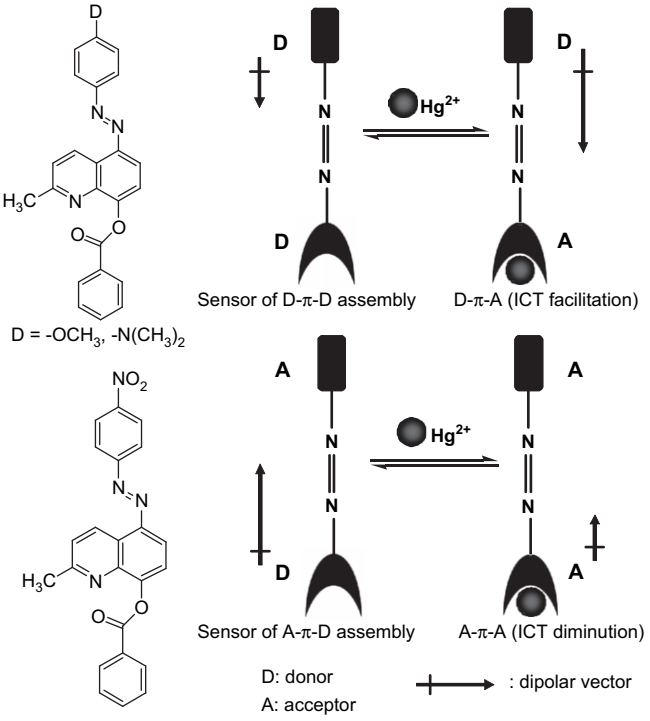

Fig. 6. The sketch of Hg^{2+} sensoring process for **2**–**4**.

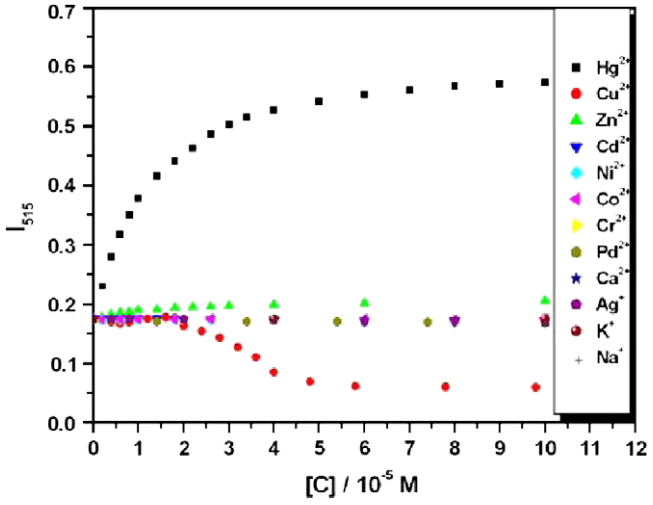

Fig. 7. Titration profiles of **3** in CH_3CN ($[C] = 2.0 \times 10^{-5}$ mol L^{-1}) with representative metal ions.

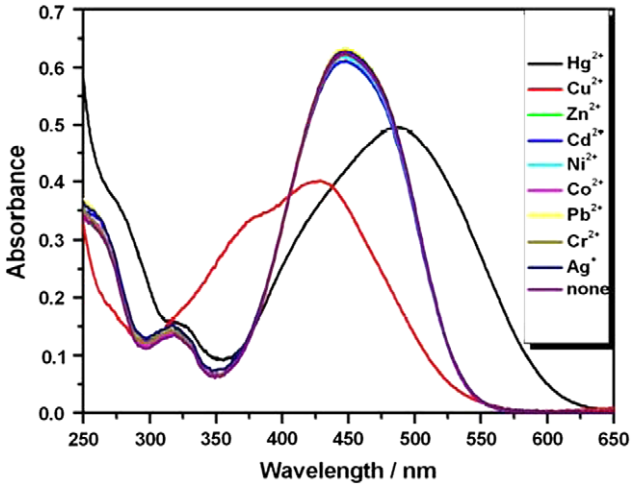

Fig. 8. UV–vis absorption spectra of **3** in $CH_3CN:H_2O = 9:1$ (v/v) ($[C] = 2.0 \times 10^{-5}$ mol L^{-1}) upon addition of 40.0 equiv. of representative metal ions.

Acknowledgment

The authors thank the National Science Foundation of China (Grant 20490210 and 20501006), Shanghai Sci. Tech. Comm. (05DJ14004 and 06QH14002) and Huo Yingdong Education Foundation (104012) for financial support.

Appendix A. Supplementary data

Crystallographic information (CIF), absorption spectra and titration profiles of compounds **1**–**4**. This material is available free of charge in the online version. Supplementary data associated with this article can be found in the online version at doi:10.1016/j.dyepig.2007.01.022.

References

[1] (a) Buhlmann P, Pretsch E, Bakker E. Chem Rev 1998;98:1593–687;
(b) Liu B, Tian H. Chem Commun 2005;3156–8;
(c) Keefe MH, Benkstein KH, Hupp JT. Coord Chem Rev 2000;205:201–28;
(d) Jiang PJ, Guo ZJ. Coord Chem Rev 2004;248:205–29;
(e) Chakrabarti A, Chawla HM, Francis T, Pant N, Upreti S. Tetrahedron 2006;62:1150–7;
(f) Basheer MC, Alex S, Thomas KG, Suresh CH, Das S. Tetrahedron 2006;62:605–10;
(g) Yang YK, Yook KJ, Tae J. J Am Chem Soc 2005;127:16760–1;
(h) Gunnlaugsson T, Leonard JP, Murray NS. Org Lett 2004;6:1557–60;
(i) Roy BC, Chandra B, Hromas D, Mallik S. Org Lett 2003;5:11–4;
(j) Sumner JP, Westerberg NM, Stoddard AK, Hurst TK, Cramer M, Thompson RB, et al. Biosens Bioelectron 2006;21:1302–8;
(k) Yang H, Liu ZQ, Zhou ZG, Shi EX, Li FY, Du YK, et al. Tetrahedron Lett 2006;47:2911–4;
(l) Zhang GX, Zhang DQ, Yin SW, Yang XD, Shuai ZG, Zhu DB. Chem Commun 2005;2161–3;
(m) Xiang Y, Tong AJ, Jin PY, Ju Y. Org Lett 2006;8:2863–6.
[2] (a) U.S. EPA. Regulatory impact analysis of the clean air mercury rule: EPA-452/R-05-003; 2005;
(b) Harris HH, Pickering IJ, George GN. Science 2004;303:764–6;
(c) Harris HH, Pickering IJ, George GN. Science 2003;301:1203;
(d) Boening DW. Chemosphere 2000;40:1335–51;
(e) Clarkson TW, Myers GJ. N Engl J Med 2003;349:1731–7.
[3] (a) Sancenon F, Martinez-Manez R, Soto J. Chem Commun 2001;2262–3;
(b) Choi MJ, Kim MY, Chang SK. Chem Commun 2001;1664–5.
[4] (a) Youn NJ, Chang SKH. Tetrahedron Lett 2005;46:125–9;
(b) Moon SY, Youn NJ, Park SM, Chang SK. J Org Chem 2005;70:2394–7;
(c) Miyake Y, Ono A. Tetrahedron Lett 2005;46:2441–3;
(d) Kim SH, Kim JS, Park SM, Chang SK. Org Lett 2006;8:371–4;
(e) Ono A, Togashi H. Angew Chem Int Ed 2004;43:4300–2;
(f) Xiao Y, Qian XH. Tetrahedron Lett 2003;44:2087–91;
(g) Guo XF, Qian XH, Jia LH. J Am Chem Soc 2004;126:2272–3;
(h) Wang Z, Zhang DQ, Zhu DB. Anal Chim Acta 2005;549:10–3;
(i) Wang JB, Qian XH, Cui JN. J Org Chem 2006;71:4308–11;
(j) Wu Z, Zhang Y, Ma JS, Yang G. Inorg Chem 2006;45:3140–2;
(k) Zhao Q, Cao TY, Li FY, Li XH, Jing H, Yi T, et al. Organometallics 2007;26:2077–81.
[5] (a) Singh LP, Bhatnagar JM. Talanta 2004;64:313–9;
(b) Liu ZT, Huan SY, Jiang JH, Shen GL, Yu RQ. Talanta 2006;68:1120–5.
[6] (a) Shi GQ, Jiang GB. Anal Sci 2002;18:1215–9;
(b) Yang YH, Wang ZJ, Yang MH, Guo MM, Wu ZY, Shen GL, et al. Sens Actuators B Chem 2006;114:1–8.
[7] Manganiello L, Rios A, Valcarcel M. Anal Chem 2002;74:921–5.
[8] (a) Zhang TZ, Anslyn EV. Org Lett 2006;8:1649–52;
(b) Chen CF, Chen QY. New J Chem 2006;30:143–7;
(c) Nazeeruddin MK, Di Censo D, Humphry-Baker R, Gratzel M. Adv Funct Mater 2006;16:189–94;
(d) Liu JW, Lu Y. Angew Chem Int Ed 2006;45:90–4;
(e) Liu ZQ, Shi M, Li FY, Fang Q, Chen ZH, Yi T, et al. Org Lett 2005;7:5481–4.
[9] (a) Ros-Lis JV, Martinez-Manez R, Rurack K, Sancenon F, Soto J, Spieles M. Inorg Chem 2004;43:5183–5;
(b) Descalzo AB, Martinez-Manez R, Radeglia R, Rurack K, Soto J. J Am Chem Soc 2003;125:3418–9;
(c) Sancenon F, Martinez-Manez R, Soto J. Tetrahedron Lett 2001;42:4321–3;
(d) Moon SY, Cha NR, Kim YH, Chang SK. J Org Chem 2004;69:181–3;
(e) Coronado E, Galan-Mascaros JR, Marti-Gastaldo C, Palomares E, Durrant JR, Vilar R, et al. J Am Chem Soc 2005;127:12351–6.
[10] Zhang H, Han LF, Zachariasse KA, Jiang YB. Org Lett 2005;7:4217–20.
[11] (a) Lee SJ, Jung JH, Seo J, Yoon I, Park KM, Lindoy LF, et al. Org Lett 2006;8:1641–3;
(b) Kano N, Yoshino J, Kawashima H. Org Lett 2005;7:3909–11;
(c) Mashhadizadeh MH, Sheikhshoaie I. Talanta 2003;60:73–80;
(d) Hassan SSM, Marzouk SAM, Sayour HEM. Talanta 2003;59:1237–44;
(e) Sands TJ, Cardwell TJ, Cattrall RW, Farrell JR, Iles PJ, Kolev SD. Sens Actuators B Chem 2002;85:33–41;
(f) Ward CJ, Patel P, James TD. Chem Lett 2001;406–7.
[12] (a) Kao TL, Wang CC, Pan YT, Shiao YJ, Yen JY, Shu CM, et al. J Org Chem 2005;70:2912–20;
(b) Li SH, Yu CW, Xu JG. Chem Commun 2005;450–2;
(c) Kim JY, Kim G, Kim CR, Lee SH, Lee JH, Kim JS. J Org Chem 2003;68:1933–7;
(d) Sancenon F, Martinez-Manez R, Soto J. Angew Chem Int Ed 2002;41:1416–9.
[13] Cheng YF, Zhao DT, Zhang M, Liu ZQ, Zhou YF, Shu TM, et al. Tetrahedron Lett 2006;47:6413–6.
[14] (a) Ho ML, Hwang FM, Chen PN, Hu YH, Cheng YM, Chen KS, et al. Org Biomol Chem 2006;4:98–103;
(b) Liu SY, He YB, Wu JL, Wei LH, Qin HJ, Meng LZ, et al. Org Biomol Chem 2004;2:1582–6;
(c) Morzumi T, Hiraga H, Nakamura H. Chem Lett 2003;32:146–7.
[15] Conners KA. Binding constants. New York: Wiley; 1987.
[16] (a) de Silva AP, Gunaratne HQN, Gunnlaugsson T, Huxley AJM, Mccoy CP, Rademacher JT, et al. Chem Rev 1997;97:1515–66;

(b) Valeur B, Leray I. Coord Chem Rev 2000;205:3–40;
(c) Liu B, Tian H. Chem Lett 2005;686–7.
[17] Huang JH, Wen WH, Sun YY, Chou PT, Fang JM. J Org Chem 2005;70: 5827–32.
[18] (a) Caballero A, Martinez R, Lloveras V, Ratera I, Vidal-Gancedo J, Wurst K, et al. J Am Chem Soc 2005;127:15666–7;
(b) Martinez R, Espinosa A, Tarraga A, Molina P. Org Lett 2005;7:5869–72.
[19] (a) Sheldrick GM. SHELXTL-Plus V5.1 software reference manual. Madison, WI: Bruker AXS Inc.; 1997;
(b) Sheldrick GM. SHELXTL-97, program for crystal structure solution. Göttingen; 1997;
(c) Sheldrick GM. SHELXTL-97, program for the refinement of crystal structures. Göttingen; 1997.
[20] Valeur B, Pouget J, Bourson J. J Phys Chem 1992;96:6545–9.